RSC Advances

ROYAL SOCIETY OF CHEMISTRY

www.rsc.org/advances

Journal Name

RSCPublishing

ARTICLE

Covalently functionalized graphene with D-glucose and its reinforcement to poly (vinyl alcohol) and poly (methyl methacrylate)

Cite this: DOI: 10.1039/x0xx00000x

Received 00th January 2012,
Accepted 00th January 2012

DOI: 10.1039/x0xx00000x

www.rsc.org/

Lu Gan[a], Songmin Shang*[a], Chun Wah Marcus Yuen[a] and Shou-xiang Jiang[a]

A chemically functionalized graphene has been synthesized by covalently grafting D-glucose onto graphene for the first time through an esterification reaction. The D-glucose functionalized graphene was further applied in the preparation of poly (vinyl alcohol) and poly (methyl methacrylate) nanocomposites. The thermal and mechanical properties of the prepared nanocomposites were then investigated. It was demonstrated that the D-glucose was grafted onto the surface of the graphene through a covalent attachment. The chemically functionalized graphene had better dispersibility in both water and dimethyl formamide than the pristine graphene. The better dispersion of the functionalized graphene in both aqueous and organic solvents simplified the preparation of the polymer nanocomposites. It was found that the D-glucose grafted graphene dispersed homogeneously in both poly (vinyl alcohol) and poly (methyl methacrylate) matrices, increasing the thermal and mechanical properties of the polymers at the same time. The phenomena were ascribed to the introduction of the D-glucose which induced a strong hydrogen bonding interactions between the functionalized graphene and the polymers. The results of this study indicate that it is an effective approach to prepare well dispersed graphene-based polymer nanocomposites by covalently attaching functional molecules onto the surface of the graphene.

1. Introduction

In recent years, nano-particles filled polymer composites have been studied intensively.[1-4] Among these nano-particle fillers, the graphene related materials have received tremendous research interest for their instinct mechanical, thermal, optical and electrical properties.[5, 6] With a 2D single layered honeycomb structure, the graphene is viewed as the thinnest, stiffest and strongest material in the world. Graphene-based composites also have found applications in various research areas such as supercapacitors,[7] catalysts,[8] sensors,[9] amongst others. In order to achieve promising properties for the graphene-based polymer composites, graphene sheets are required to disperse homogeneously within the matrices. However, it is very difficult to obtain well exfoliated graphene sheets with single or few layers in both solvents and polymers due to the strong intermolecular van der Vaals forces among them.[10] Hence, unless some pre-treatments to the graphene are made, it is almost impossible to prevent graphene sheets aggregations. Physically blending or adsorbing some molecules like surfactants [11] and polymers,[12] onto the surface of the graphene sheets could improve graphene dispersion effectively. These foreign molecules act as the compatibilizer to weaken the van der Vaals forces among the graphene sheets. Meanwhile, these compatibilizers more or less attenuate the reinforcing effect of the graphene despite the fact that individual graphene sheets could be observed in the nanocomposites.

Due to this reason, researchers are exploring the possibility of chemical functionalization to graphene. As a significant precursor and derivative of the graphene, the graphene oxide (GO) tends to be more compatible with some solvents [13] and polymers [14] since the GO consists of many oxygen containing groups compared with the graphene.[15] These groups further facilitate the chemical modifications on the GO. Through simple organic reactions, the GO is able to be covalently bonded with some small molecules [16] or polymers,[17, 18] and these chemically functionalized graphene (CFG) molecules are more dispersible in aqueous [19] and organic [20] solvents, and polymer matrixes.[21] Moreover, the CFGs are more easily incorporated into the polymer without losing the inherent properties of the CFGs and the prepared nanocomposites.[22] Recently, much interest has arisen towards synthesizing solvents dispersible or soluble CFGs.[23, 24] Long time stable CFG dispersions simplify the fabrication of the polymer composites through solvents mixing approaches.

As a most common and simple monosaccharide, the D-glucose has been widely used in biology, pharmacy and clinical related areas for centuries.[25] It is also the basic nutrient for almost all organisms. More significantly, the D-glucose has a number of hydroxyl and aldehyde groups along its backbone and was soluble in water and many organic solvents like dimethyl formamide (DMF) and pyridine. If the D-glucose could be covalently grafted onto the graphene,[26] the D-glucose grafted CFG is expected to have better dispersion in both aqueous and organic solvents, which is very important for preparing

polymer nanocomposites. Compared with those CFGs which could only disperse in either aqueous or organic solvents, the D-glucose grafted CFG has wider application potentials for more polymer matrices. Moreover, this D-glucose grafted CFG is expected to have stronger interactions with the polymers, especially those with oxygen containing groups like poly (vinyl alcohol) (PVA) and poly (methyl methacrylate) (PMMA) since the existence of the D-glucose will facilitate the hydrogen bonding interactions between the CFG and the polymers.

Herein, this study first reported the attachment of the graphene and the D-glucose through covalent grafting. The D-glucose grafted graphene, named as Glu-G, was further incorporated into the PVA and the PMMA to prepare their nanocomposites. Fourier transform infrared (FTIR), thermogravimetric analysis (TGA), RAMAN spectroscopy and X-ray diffraction (XRD) were used to confirm the structure of the Glu-G. The dispersions of the Glu-G in water and DMF were also investigated. In order to study the reinforcing effect of the Glu-G to the polymers and the interaction between the fillers and the matrices, the PVA/Glu-G and the PMMA/Glu-G nanocomposites were characterized by morphological, mechanical and thermal properties, respectively.

2. Experimental

2.1 Materials

Natural graphite flake, hydrazine hydrate ($N_2H_4{\cdot}H_2O$), 4-dimethyl aminopyridine (DMAP, 99%), and N,N-dicyclohexylcarbo-diimide (DCC) were purchased from Aldrich (America). PVA (Mw ~ 70,000 – 85,000, ~87-89% alcoholized) was purchased from Accuchem (Canada). PMMA (Mass Density 1.19 g/cm^{-3}, Hardness ~148 N/mm^2) was purchased from International Laboratory (America). D-glucose was purchased from Unichem (China). All the other agents and solvents were of analytical grade and used as received. Deionized-distilled water (DDW) was used exclusively in this study.

2.2 Synthesis of D-Glucose grafted Graphene (Glu-G)

GO was synthesized by the modified Hummer Method reported previously.[27] The synthesis of the Glu-G followed an esterification procedure in the presence of DMAP and DCC as follows. Purified GO (50 mg) was dissolved in dimethyl sulfoxide (DMSO, 20 mL) by sonication for 1 h and gently stirring for another 30 min. DCC (2.0 g, 9 mmol) and DMAP (0.15 g, 1.3 mmol) were then added gradually into the solution. After another 30 min of stirring, the D-glucose (0.4 g, 2.2 mmol) dissolved in 10 mL DMSO was added to the solution and the resulting mixture was stirred at 60 ^oC for 4 days. Methanol (200 mL) was added to the mixture thereafter and the suspension was filtered and washed with acetone (300 mL). In order to completely remove the non-reacted GO and D-glucose, the residue was washed with hot water and filtered. After this step was processed for 3 times, the resulting solid, named as Glu-GO, was dissolved in 30 mL DDW by sonication for 1 h. After 2 mL of hydrazine hydrate was added, the solution was heated to 60 ^oC for 10 h with stirring. Then the suspension was filtered through a PTFE membrane and the residue was washed with methanol (3×20 mL) and hot water (3×20 mL). Finally, the Glu-G was dried in the vacuum oven at 60 ^oC for 24 h. The scheme of the reaction formula is shown in Fig. 1.

2.3 Preparation of Glu-G/PVA nanocomposite

Glu-G (50 mg) was first dissolved in DDW (100 mL) and sonicated for 2 h. At the same time, PVA (0.5 g) was put into 50 mL DDW and heated at 85 ^oC for 1 h with continuous stirring. After a clear PVA solution was obtained, Glu-G solution was dropwise added into the solution. After all the Glu-G solution was added, the mixture was stirred at room temperature for another 30 min. The mixture was then poured into a glass dish and kept at room temperature until the weight was constant. Finally, the PVA/Glu-G 1.0 wt% film was obtained. For comparison, pure PVA film was also prepared following the similar procedures.

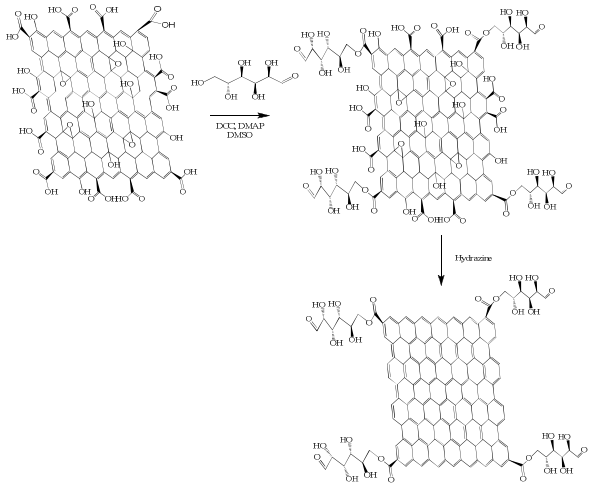

Fig.1. Scheme of the reaction formula for synthesizing Glu-G.

2.4 Preparation of Glu-G/PMMA nanocomposite

Glu-G (50 mg) was first dissolved in DMF (100 mL) and sonicated for 1 h to get a homogeneous dispersion. At the same time, PMMA (0.5 g) was dissolved in DMF (20 mL) with continuous stirring. Thereafter, the Glu-G dispersion was added into the PMMA solution and the resulted suspension was sonicated for another 1 h. The Glu-G/PMMA suspension was then transferred to a glass dishes and kept at 100 ^oC until the weight was constant. In order to totally remove the residue DMF, the film was dried in the vacuum oven at 100 ^oC for another 24 h. Finally, the PMMA/Glu-G 1.0 wt% film was obtained. For comparison, pure PMMA film was also prepared with similar procedures.

2.5 Characterization

FTIR spectra were recorded using a Perkin Elmer 100 spectrophotometer with a resolution of 4 cm^{-1} and 16 scans. TGA was carried out using a Mettler Toledo TGA 1 Simultaneous Thermal analyser with the temperature increasing from 25 to 800 ^oC at a heating rate of 10 ^oC/min. RAMAN spectra were performed using a Horiba Jobin Yvon HR800 Raman spectrometer, which was equipped with an Ar laser (487.97 nm, 180 mW) as the excitation light source, and an Olympus BX41 microscope. UV-vis absorption spectra were recorded with a Biochrom Libra S35 UV/Vis Spectrophotometer from 200 to 800 nm. The X-ray diffraction (XRD) was performed using Cu Kα radiation source (1.54 Å) in a Rigaku Smartlab XRD instrument. Transmission electron microscopy (TEM) images of the Glu-G were recorded using a Jeol JEM-2100F TEM instrument operated at 200 kV. The atomic force microscopy (AFM) image of the Glu-G was investigated by a Bruker

Nanoscope 8 SPM instrument using a tapping mode. Scanning electron microscopy (SEM) was conducted by the JEOL SEM 6490 to examine the fracture surface the polymer matrices and their nanocomposites. The samples were coated with a thin layer of gold before observation. Differential scanning calorimetry (DSC) was carried out using a Perkin Elmer Pyris 1 DSC analyzer under nitrogen atmosphere. A universal tensile testing machine, Instron 5566, was used to test the mechanical properties. The testing was operated at room temperature with a cell load of 500 N, and the gauge length was 20 mm and extension rate was 5 mm min^{-1}. The samples were cut into ribbon like shape of 60×5×0.1 mm before testing.

3. Results and Discussions

3.1 Characterization of Glu-G

The formation of the Glu-G was characterized first by FTIR spectra shown in Fig. 2(a). It could be seen that after the GO was grafted with the D-glucose (which is Glu-GO), a new peak at around 1735 cm^{-1} (C=O stretching vibration) appeared and the intensity of the original peak at 1705 cm^{-1} became weaker, indicating that some carboxylic acid groups presented in the GO had been transferred to the ester groups. After the Glu-GO was reduced to the Glu-G, the peak at 1705 cm^{-1} disappeared and ~1100 cm^{-1} (C-O-C stretching vibration) became weaker, indicating the unreacted -COOH groups and the epoxy groups were eliminated by the hydrazine (see Fig. 1). Besides, the intensity of the two peaks at around 2900 cm^{-1} (-CH- stretching vibration) increased largely, indicating that the resulting product contained more CH groups (on the glucose backbone). The peak intensity at around 3100 to 3500 cm^{-1} (-OH stretching vibration) was still relatively strong, indicating that the grafted D-glucose was not affected by the hydrazine much.

TGA being carried out in a nitrogen atmosphere was then used to investigate the grafting rate of Glu-G as shown in Fig. 2(b). It could be seen from the curves that the percentage weight of loss was about 40% for GO and 52% for Glu-GO at 600 ^{o}C. Based on this result, it was calculated that there was about 23 wt% of glucose and 77 wt% of GO in the Glu-GO. After the Glu-GO was reduced to the Glu-G, the weight loss percentage of the Glu-G at 600 ^{o}C was about 25%. Since the oxygen containing groups had been eliminated through reducing process,[28] the weight loss of the Glu-G was mainly the D-glucose. Since the weight contents of the D-glucose obtained from the results from Glu-GO and Glu-G were similar, it was confirmed that D-glucose was grafted onto the graphene and the grafting rate was ~20%.

It has been well known that the oxidation of graphite destroys partially the sp^2 structure of the graphite. Thus, RAMAN spectroscopy was conducted to detect the structure deformation and Fig. 2(c) presents the RAMAN spectra of the GO，the Glu-GO and the Glu-G. It could be observed that all three materials had two characteristic peaks at around 1350 cm^{-1} and 1580 cm^{-1}, which were generally named as the D band and G band. The D band indicates the carbons with sp^3 hybridization while the G band represents for sp^2 hybridized carbons. The intensity ratio of these two bands (I_D/I_G) is often introduced to speculate the degree of the structure defect. From Fig. 2(c), it was calculate that I_D/I_G for GO was about 0.86. After the D-glucose was covalently attached to the GO, the G band red shifted to 1572 cm^{-1} and the I_D/I_G for the Glu-GO was a lower (0.80) compared with that of the GO. The sp^2 domains increased during the reaction process, resulting in the decrease of the I_D/I_G ratio. When the Glu-GO turned to the Glu-G after a reduction process, an increase of I_D/I_G (1.09) was observed, indicating that the reduction decreased the topological disorder of the graphene due to the removal of the oxygen groups.[29] The peaks at around 2700 cm^{-1} was known as the 2D band of the carbon materials. It was also observed from Fig.2(c) that although the peak position of the Glu-G at 2D band shifted a little, the peak intensity of the Glu-G was almost the same as the GO, indicating that Glu-G could be also exfoliated to a few layers in the solvents.

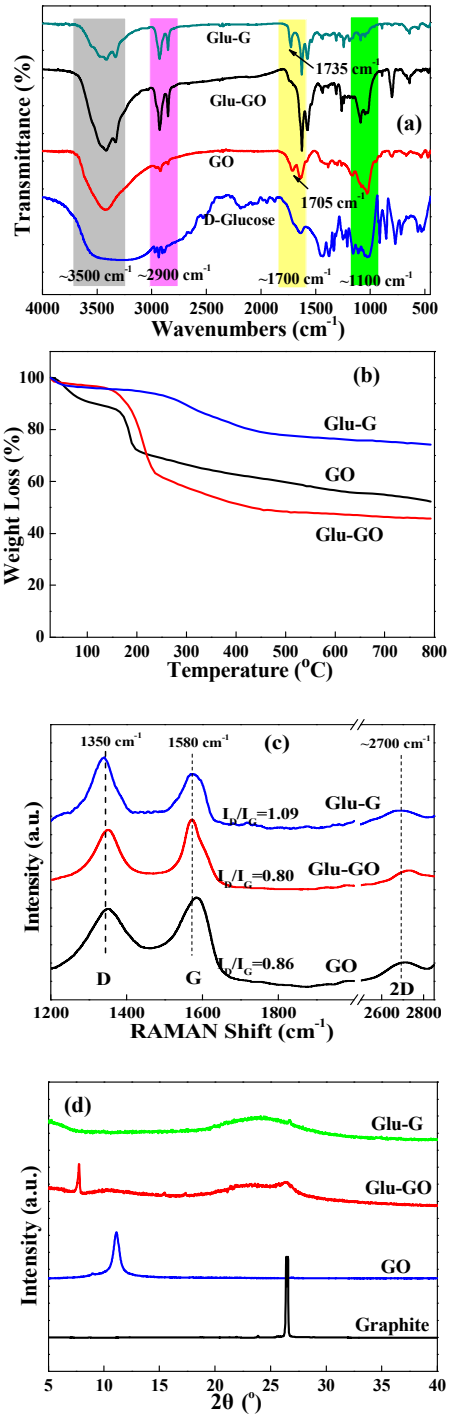

Fig.2. (a) FTIR spectra; (b) TGA curves (under nitrogen); (c) RAMAN spectra and (d) XRD patterns of GO, Glu-GO and Glu-G

Fig. 2(d) shows the XRD patterns of graphite, GO, Glu-GO and Glu-G. It could be seen that the graphene had a characteristic peak at ~26° (002) with a d spacing of 0.34 nm.[30] After oxidation, the GO had a characteristic peak at ~11° (001) with a much larger d spacing of 0.81 nm, due to the existence of the oxygen groups. After D-glucose was grafted onto the GO, the peak of the Glu-GO shifted to lower value, indicating that the introduction of the D-glucose gave rise to the interlayer spacing of the graphene sheet. The Glu-G had a broad peak at ~24° (002), which meant the covalent attachment of the D-glucose did not destroy the crystalline structure of the graphene.

Fig. 3(a) and 3(b) shows the TEM images of the Glu-G. It could be observed that the Glu-G was able to be exfoliated to very few layers. The selected area electron diffraction (SAED) pattern of the Glu-G showed well-defined diffraction spots, indicating a crystalline structure of the reduced Glu-G. Fig. 3(c) gives the UV absorption spectra of the GO and the Glu-G in water (with the concentration of 0.05 mg/mL). It has been well known that the absorption peak λ_{max} represents for the π conjugation of the investigated material. Compared with that of the GO (~220 nm), the λ_{max} of the Glu-G (~280 nm) had a red shift to higher value, indicating that the conjugation system of the Glu-G was restored after the reduction process.[31]

The introducing of the D-glucose to the surface of the graphene also affects the dispersibility of the functionalized graphene. Since the D-glucose contains a number of oxygen containing groups along its backbone, the Glu-G had a much better dispersibility than GO in both aqueous and organic solvents. As shown in Fig. 3(d), the Glu-G was able to disperse in water and DMF homogeneously without aggregation for more than 2 months. The UV-vis spectra of the Glu-G in water and DMF were shown in Fig. 3(e) and Fig. 3(f). From the inset figures, it could be seen that the Glu-G solution in both water and DMF obeyed the Beer's law. Following Beer's law, the extinction coefficient for the Glu-G in water was 36.4mL/mg·cm, with a maximal solubility of 0.58 mg/mL, and the extinction coefficient for the Glu-G in DMF was 42.2 mL/mg·cm, with a maximal solubility of 0.61 mg/mL. The good dispersion of Glu-G in both aqueous and organic solvents facilitates the fabrication of the Glu-G based nanocomposites for both aqueous soluble and organic soluble polymers.

The surface morphology of the GO and the Glu-G was then investigated by AFM shown in Fig. 4. As could be seen from the height profile, the GO had an average thickness of ~1.0 nm, which was accordant with the previous studies.[32] On the other hand, the Glu-G sheet had an average thickness of ~3.2 nm, which is much thicker than that of the GO. This result was mainly ascribed to the introduction of the D-glucose on to both sides of the graphene sheets and the grafted D-glucose contributed the thickness of the Glu-G.

3.2 Characterization of Glu-G/PVA and Glu-G/PMMA Nanocomposites

The structures of the Glu-G/PVA and the Glu-G/PMMA nanocomposites were first characterized in terms of morphology of fracture surface by SEM shown in Fig. 5(a) and 5(b). It could be clearly observed that the surfaces of both PVA/Glu-G and PMMA/Glu-G presented a uniformly layered structure. Besides the homogeneous dispersion of the Glu-G in the polymer matrices, the Glu-G sheets also tended to distribute in parallel with the same directions in the polymers. The well distributed Glu-G in the polymer matrices indicated that the Glu-G had very well-bonded interactions with both PVA and PMMA.

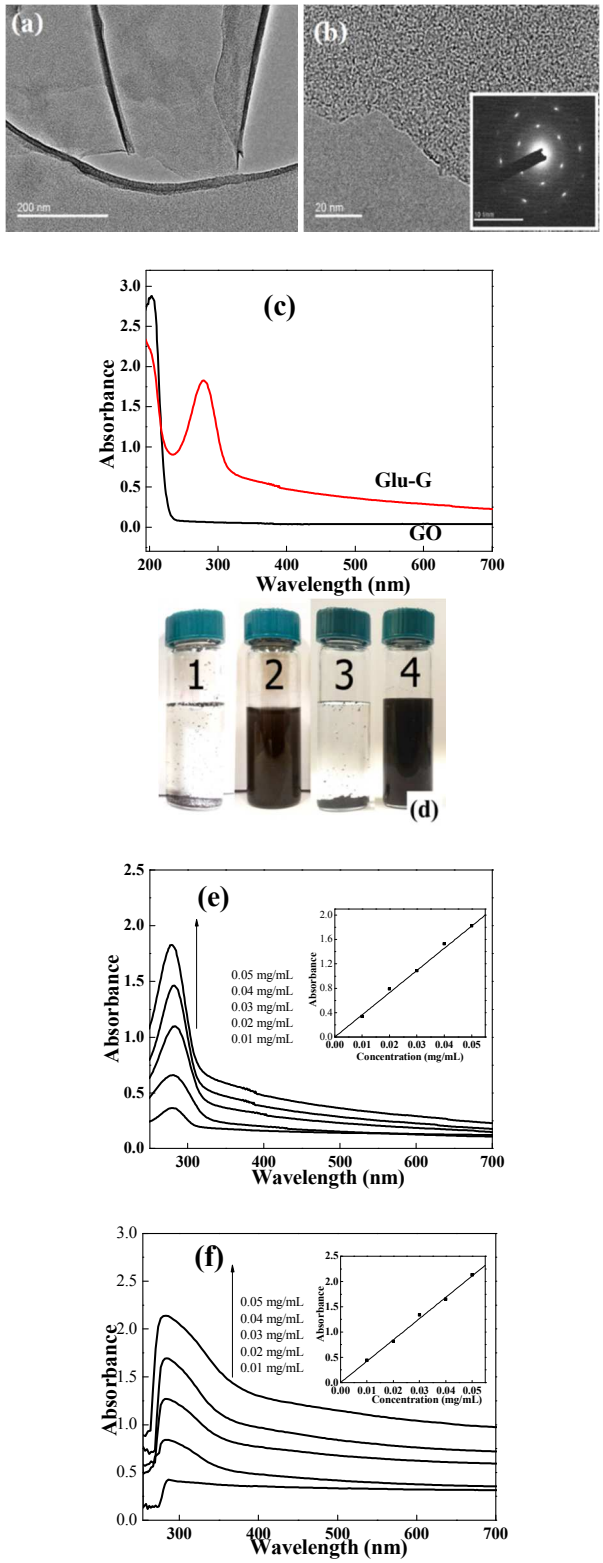

Fig. 3. (a) TEM, (b) high resolution TEM images of the Glu-G; (c) UV-vis spectra of the 0.05 mg/mL Glu-G and GO solutions; (d) digital pictures of graphene dispersions in (1) water and (3) DMF; and Glu-G dispersions in (2) water and (4) DMF; UV–Vis spectra of Glu-G in (e) water and(f) DMF at different concentrations. The insets show the relationship between the absorbance and the concentration of the Glu-G

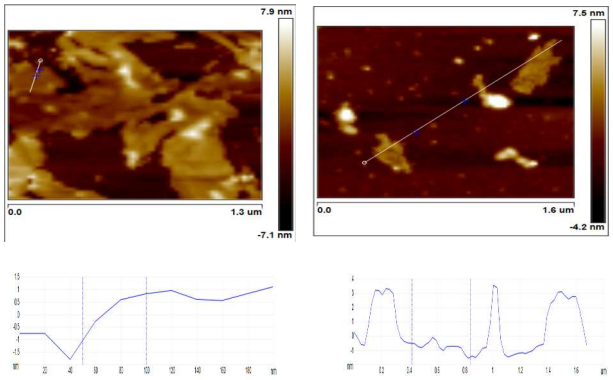

Fig.4 AFM image of GO (Left) and Glu-G (Right)

To further investigate the structure of the nanocomposites, XRD analysis was conducted and the results were shown in Fig. 5(c). It was observed that pure PVA showed characteristic peaks at ~20°, which was corresponding to the crystalline phase of the PVA. The PMMA had two very broad peaks at ~14.5° and ~30°, revealing its amorphous structure.[33] After Glu-G was incorporated, the peaks of the resulting nanocomposites were almost the same as the pristine polymers, suggesting that Glu-G sheets were fully exfoliated and well dispersed without changing the structure of the polymer matrices.

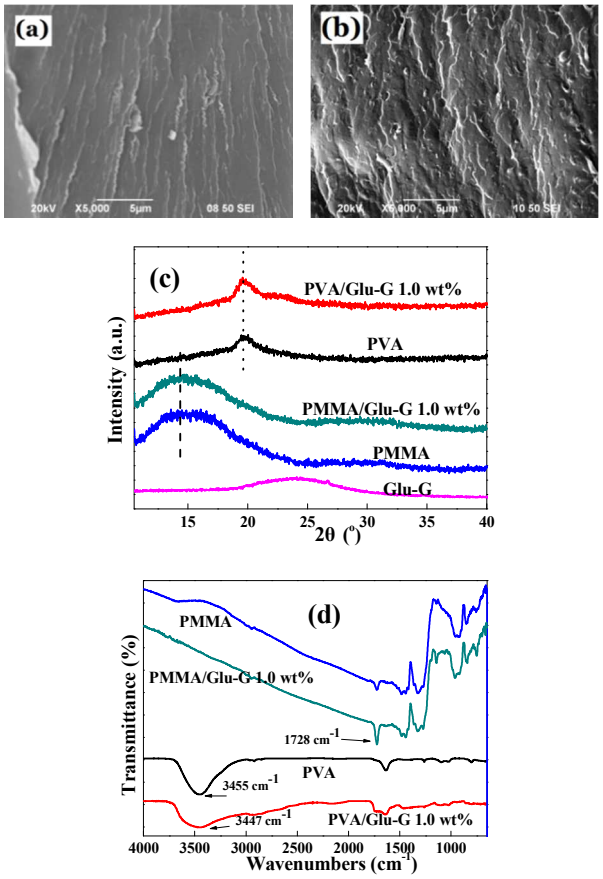

Fig.5. SEM images of the fractured surface of (a) PVA/Glu-G and (b) PMMA/Glu-G nanocomposites; (c) XRD patterns and (d) FTIR spectra of PVA, PMMA and their nanocomposites.

It was believed that strong interactions between the Glu-G and the polymers resulted in a uniform dispersion of the Glu-G and the interactions were confirmed by the FTIR spectra as shown in Fig. 5(d). Take the PVA and the PVA/Glu-G as an example, it was seen that pure PVA had a wide band at ~3455 cm^{-1}, which was attributed to the stretching vibration of the O-H bond. When the Glu-G was incorporated into the PVA, the peak became broader and shifted to a lower wavenumber at ~3447 cm^{-1}. This was due to the strong interactions between the Glu-G and the PVA. Since the D-glucose had a number of oxygen containing groups like formyl and hydroxyl groups, the Glu-G was able to form interactions through hydrogen bonding with –OH groups along the PVA chains, resulting in the shift of -OH in FTIR spectra. Analogously, the Glu-G also formed hydrogen bond with the PMMA due to the existence of the methyl ester groups within the PMMA backbone. It could be seen from the spectra that the intensity at ~1728 cm^{-1} (C=O stretching vibration) in the PMMA/Glu-G nanocomposite increased compared to that of the pristine PMMA, which might resulted from the interactions between the –OH groups in the Glu-G and the $COOCH_3$ groups in the PMMA. The schematic illustration of the interactions between the filler and the matrices was thus shown in Fig. 6. Unlike pristine graphene, since the Glu-G contains the D-glucose within its body, the Glu-G is more dispersible in both solvents and polymers than the pristine graphene without introducing foreign compatibilizers. It is thus expected that the synthesized Glu-G is a good reinforcing filler for polymers with oxygen-containing and nitrogen-containing groups like polyurethane (PU), resin, etc.

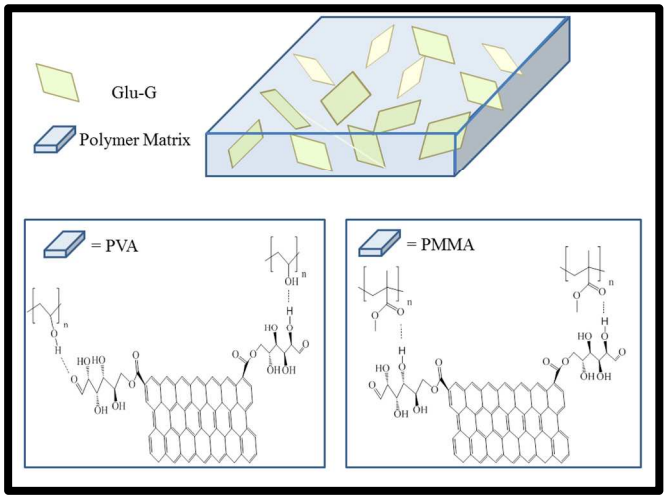

Fig. 6. Schematic illustrations of the interactions between the filler and the matrices

3.3 Thermal and Mechanical Properties of Glu-G/PVA and Glu-G/PMMA nanocomposites

The glass transition temperatures of the PVA, PMMA and their nanocomposites were investigated by DSC with the results shown in Fig. 7(a) and 7(b). Compared with that of the pure polymer, the glass transition temperature (T_g) of the PVA/Glu-G nanocomposite increased from 66.8 to 69.1 °C, and the T_g of the PMMA/Glu-G nanocomposite increased from 118.7 to 120.4 °C. The increased T_g of the resulting nanocomposites was ascribed to the uniform dispersion of the Glu-G in the polymer matrices and the strong hydrogen bonding between them, which was accord with some previous studies.[34, 35] The TGA measurement being carried out in air atmosphere was further conducted with the results shown in Fig. 7(c) and 7(d). It was clearly seen that the nanocomposites were much more thermally stable than the pure polymers. For example, the

degradation temperatures at 20% weight loss of both the PVA/Glu-G and the PMMA/Glu-G nanocomposites were higher than their pristine polymers. The improved thermal stability of the Glu-G filled nanocomposites was also ascribed to the good interactions between the Glu-G and the polymers.

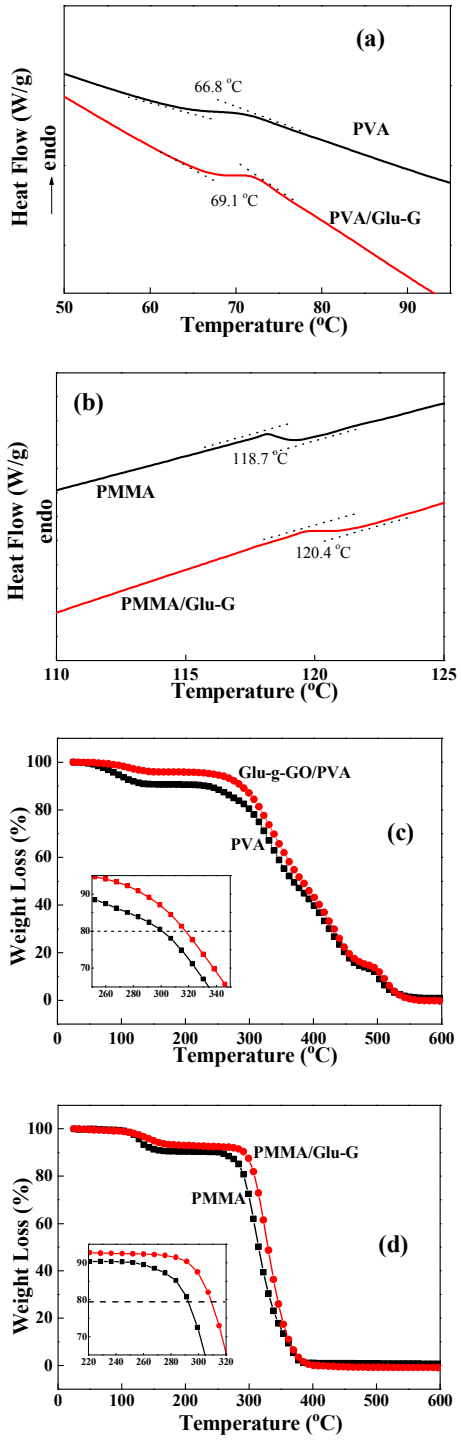

Fig.7. DSC curves of (a) PVA, PVA/Glu-G nanocomposite, and (b) PMMA and PMMA/Glu-G nanocomposite; and TGA curves of (c) PVA, PVA/Glu-G nanocomposite, and (d) PMMA and PMMA/Glu-G nanocomposite.

It was well known that the mechanical properties of a polymer could be influenced tremendously by the nanofillers incorporated into its matrix.[36, 37] Hence, a typical stress-strain test was conducted with the results shown in Fig. 8 (a), 8(b) and Table 1. It was clearly observed that the incorporation of the Glu-G notably improved the mechanical strength of the PVA and PMMA. Although the elongation of the nanocomposites decreased slightly, the Young's modulus and the tensile stress of both the PVA and the PMMA nanocomposites improved significantly compared to that of the pristine polymers (Table 1). The incorporation of the Glu-G decreased the crystallinity of the polymers. The decrease in polymer crystallinity made the prepared nanocomposites tougher and easier to be broken down, which caused a slight decrease in the elongation of the nanocomposites. However, the strong hydrogen boding interactions between the Glu-G and the polymers facilitated an effective load transfer from the polymer matrices to the filler when the nanocomposites were under stretching force, resulting in the improvement in the Young's modulus and the tensile stress.

Table 1. Tensile properties of the PVA, PMMA and their nanocomposites.

Samples	Tensile Stress (MPa)	Tensile Strain (%)	Modulus (MPa)
PVA	18.4	71.7	526
PVA/Glu-G 1.0 wt%	25.1	70.3	808
PMMA	43.1	4.6	14.9
PVA/Glu-G 1.0 wt%	46.6	3.5	21.2

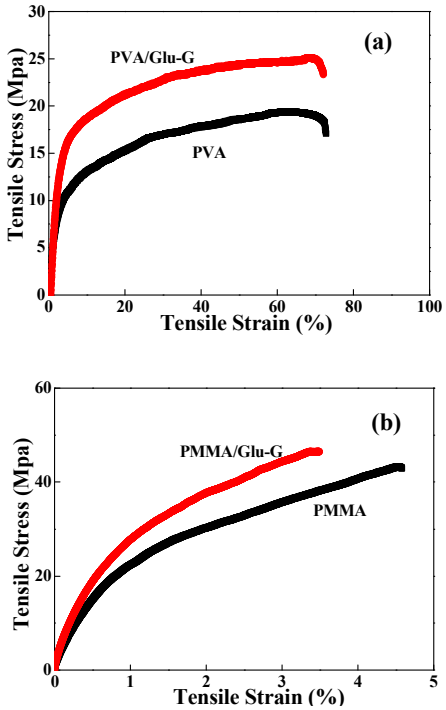

Fig. 8. Stress-strain curves of (a) PVA, PVA/Glu-G nanocomposite, and (b) PMMA and PMMA/Glu-G nanocomposite

4. Conclusions

In conclusion, the D-glucose was covalently attached to the graphene and the grafting rate was about 20%. The functionalized graphene had good dispersibility in both aqueous and organic solvents like water and DMF. The introduction of the D-glucose also improved the affinity of the functionalized graphene and the polymers such as PVA and PMMA. Based on the XRD and SEM results, it was investigated that the Glu-G dispersed within both the PVA and PMMA matrices homogeneously and Glu-G sheets tended to align parallelly with the same direction. It was then found that the Glu-G interacted with the polymers through hydrogen bonding. The good interactions between the filler and the matrices also improved the mechanical and thermal properties of the polymers, which were validated by DSC, TGA and mechanical testing. The results suggest that the synthesized Glu-G is a desirable reinforcing nanofillers for polymers with oxygen-containing and nitrogen-containing groups. The interactions between the Glu-G and the polymers could effectively improve the thermal and mechanical properties of the matrix polymers. Compared with those CFGs which could only disperse in either aqueous or organic solvents, the Glu-G synthesized in this study has wider application potentials for more polymer matrices.

Acknowledgements

The work was supported by the General Research Fund (Project No. 532712) of the Research Grants Council of Hong Kong and The Hong Kong Polytechnic University scholarship.

Notes and references

[a] Institute of Textiles and Clothing, The Hong Kong Polytechnic University, Hong Kong. Tel.: + 852 3400 3085; fax: + 852 2773 1432
E-mail addresses: shang.songmin@polyu.edu.hk (SM Shang)

1 W. Zeng, X. Tao, S. Chen, S. Shang, H. Chan and A. S. Choy, *Energy Environ. Sci.*, 2013, **6**, 2631-2638.
2 Y. Xu, S. M. Shang and J. Huang, *Polym. Test.*, 2010, **29**, 1007-1013.
3 S. M. Shang, L. Gan and M. C. W. Yuen, *Compos. Sci. Technol.*, 2013, **86**, 129-134.
4 S. M. Shang, W. Zeng and X. M. Tao, *Sens. Actuator B-Chem.*, 2012, **166**, 330-337.
5 Q. Zhang, J. Pan, X. Yi, L. Li and S. M. Shang, *Org. Electron.*, 2012, **13**, 1289-1295.
6 Y. Zeng, L. Qiu, K. Wang, J. Yao, D. Li, G. P. Simon, R. Wang and H. Wang, *RSC Adv.*, 2013, **3**, 887-894.
7 R. S. Diggikar, D. J. Late and B. B. Kale, *RSC Adv.*, 2014, 4, 22551-22560.
8 J. Zhao, L. Zhang, H. Xue, Z. Wang and H. Hu, *RSC Adv.*, 2012, 2, 9651-9659.
9 S.M. Shang, L. Gan, M. C.W. Yuen, S.X. Jiang and N. M. Luo, *Compos. Part A-Appl. S.*, 2014, **66**, 135-141.
10 W. Ai, J.-Q. Liu, Z.-Z. Du, X.-X. Liu, J.-Z. Shang, M.-D. Yi, L.-H. Xie, J.-J. Zhang, H.-F. Lin, T. Yu and W. Huang, *RSC Adv.*, 2013, **3**, 45-49.
11 J. Guo, L. Ren, R. Wang, C. Zhang, Y. Yang and T. Liu, *Compos. Part B-Eng.*, 2011, **42**, 2130-2135.
12 J. Wang, J. Wu, W. Xu, Q. Zhang and Q. Fu, *Compos. Sci. Technol.*, 2014, **91**, 1-7.
13 N. Y. Yuan, F. F. Ma, Y. Fan, Y. B. Liu and J. N. Ding, *Compos. Part A-Appl. S.*, 2012, **43**, 2183-2188.
14 O. J. Yoon, C. Y. Jung, I. Y. Sohn, H. J. Kim, B. Hong, M. S. Jhon and N.-E. Lee, *Compos. Part A-Appl. S.*, 2011, **42**, 1978-1984.
15 D. Spasevska, V. Daniloska, G. P. Leal, J. B. Gilev and R. Tomovska, *RSC Adv.*, 2014, **4**, 24477-24483.
16 D. W. Boukhvalov, *RSC Adv.*, 2013, **3**, 7150-7159.
17 B. Shen, W. Zhai, M. Tao, D. Lu and W. Zheng, *Compos. Sci. Technol.*, 2013, **77**, 87-94.
18 Y. Mo, M. Yang, Z. Lu and F. Huang, *Compos. Part A-Appl. S.*, 2013, **54**, 153-158.
19 B. Shen, W. Zhai, D. Lu, J. Wang and W. Zheng, *RSC Adv.*, 2012, **2**, 4713-4719.
20 O.-K. Park, S.-G. Kim, N.-H. You, B.-C. Ku, D. Hui and J. H. Lee, *Compos. Part B-Eng.*, 2014, **56**, 365-371.
21 C. Deetuam, C. Samthong, S. Thongyai, P. Praserthdam and A. Somwangthanaroj, *Compos. Sci. Technol.*, 2014, **93**, 1-8.
22 K. Liu, S. Chen, Y. Luo, D. Jia, H. Gao, G. Hu and L. Liu, *Compos. Sci. Technol.*, 2013, **88**, 84-91.
23 W. Yu, J. Fu, X. Dong, L. Chen and L. Shi, *Compos. Sci. Technol.*, 2014, **92**, 112-119.
24 E. Ou, Y. Xie, C. Peng, Y. Song, H. Peng, Y. Xiong and W. Xu, *RSC Adv.*, 2013, **3**, 9490-9499.
25 C. T. Wass and W. L. Lanier, *Mayo .Clin. Proc.,* 1996, **71**,801-812.
26 K. P. Loh, Q. Bao, P. K. Ang and J. Yang, *J. Mater. Chem.*, 2010, **20**, 2277-2289.
27 L. Y. Li, K. Q. Xia, L. Li, S. M. Shang, Q. Z. Guo and G. P. Yan, *J. Nanopart. Res.*, 2012, **14**, 908.
28 S. Chandrasekaran, G. Faiella, L. A. S. A. Prado, F. Tölle, R. Mülhaupt and K. Schulte, *Compos. Part A-Appl. S.*, 2013, **49**, 51-57.
29 T. Kuila, S. Bose, P. Khanra, N. H. Kim, K. Y. Rhee and J. H. Lee, *Compos. Part A-Appl. S.*, 2011, **42**, 1856-1861.
30 H. Yang, C. Shan, F. Li, D. Han, Q. Zhang and L. Niu, *Chem. Commun.*, 2009 , **26**, 3880-3882.
31 D. Li, M. B. Mueller, S. Gilje, R. B. Kaner and G. G. Wallace, *Nat. Nanotechnol.*, 2008, **3**, 101-105.
32 C. Xu, J. Gao, H. Xiu, X. Li, J. Zhang, F. Luo, Q. Zhang, F. Chen and Q. Fu, *Compos. Part A-Appl. S.*, 2013, **53**, 24-33.
33 Y. Li, B. Zhang and X. Pan, *Compos. Sci. Technol.*, 2008, **68,** 1954-1961.
34 X. M. Yang, L. Li, S. M. Shang and X. M. Tao, *Polymer*, 2010, **51**, 3431-3435.
35 J. Shen, B. Yan, T. Li, Y. Long, N. Li and M. Ye, *Compos. Part A-Appl. S.*, 2012, **43**, 1476-1481.
36 S. Biswas, H. Fukushima and L. T. Drzal, *Compos. Part A-Appl. S.*, 2011, **42**, 371-375.
37 S. C. Shiu and J. L. Tsai, *Compos. Part B-Eng.*, 2014, **56**, 691-697.